The Implantation Profiles of 10, 20 and 40 keV ^{85}Kr in Gallium Arsenide

J. L. WHITTON,* G. CARTER
Department of Electrical Engineering, University of Salford, Salford, Lancs, U K

J. H. FREEMAN, G. A. GARD
Atomic Energy Research Establishment, Harwell, Berks, U K

Received 26 August 1968, and in revised form 12 November

The possibility of making semiconductor devices by implantation of impurity atoms requires a knowledge of their depth distribution or implantation profile. The use of a micro-mechanical sectioning technique has made such measurements possible over depths of as small as 30 Å. These measurements have been made as a function of incident energy, crystallographic direction and bombardment dose of radioactive krypton in single crystals of GaAs.

It is concluded that the ion implantation of GaAs is a viable process, that GaAs suffers ion bombardment induced damage at a relatively low dose and that the energy and orientation dependence are similar to those seen previously in face-centred cubic materials.

1. Introduction

The method of forming semiconductor devices by ion implantation has several advantages over the more conventional diffusion techniques, not the least of which is the possibility of a high degree of control over the implantation profile. This has already been demonstrated by the introduction of active dopant ions into silicon [1, 2] and is expected to be of more useful application in the III-V compounds where, because of problems of dissociation and complex diffusion processes, the possibility of diffusing dopant ions in a well-controlled and reproducible fashion is remote.

The control of the implantation profile can be achieved by a proper choice of incident energy, or combination of energies of the dopant ion, which may be directed into certain channelling or non-channelling directions of the target crystal lattice. However, before useful programming of the implantation conditions can be made, it is necessary to know the range and depth distribution of the dopant in the target crystal as a function of incident energy, bombardment dose, ion type and crystallographic direction.

Although it would be valuable to be able to predict reasonably accurately the depth distribution as a function of these parameters, this is not yet possible. Present theory [3, 4] which is adequate for the prediction of various ion ranges in amorphous target material where collisions may be considered as random events, is not yet at the stage which can take into account the channelling effect due to the periodicity of the lattice nor the very deep diffusion controlled penetration seen for many ions in tungsten [5].

The oscillating dependence of electronic stopping processes on the atomic number of the incident ion is not sufficiently well understood to be completely predictable [6] although a recent theoretical interpretation appears to adequately fit the available experimental data; similarly the different modes of penetration observed in for instance, gold and tungsten, although believed due to a combination of atomic thermal vibrational amplitudes and effective densities of the incident ions [7], are not yet predictable.

It appears therefore, that to adequately programme the ion implantation of semiconductor devices, it is, at least for the present,

*Permanent address: Research Chemistry Branch, Atomic Energy of Canada Ltd, Chalk River, Ontario, Canada.

AECL-3596

mandatory to first of all make careful experimental measurements of the implantation profiles obtained under precisely controlled conditions. That this has not been done for the semiconductors of the III-V series is because until recently, no acceptable method of measuring these profiles had been developed.

The most direct method of measuring implantation profiles is that of injecting a suitable radiotracer into the crystal, removing successive layers and measuring the activity remaining in the crystal after each layer is removed. The information obtained gives the integral depth distribution of the radioactive atoms in the crystal.

The requirements for sectioning techniques are rather stringent, as they should be capable of removing layers uniformly, reproducibly and of a thickness that is small (i.e. some tens of Å) compared to the range of the incident ions. The various techniques developed to date are, (a) anodic oxidation/dissolution for W, Al, Si and Au [8-11], (b) corrosive film formation for Au, Pb and Sn [12], (c) chemical dissolution for NaCl and KBr [13], (d) low energy sputtering for Cu [14], Au [15] and GaAs [16] and (e) vibratory polishing for W, Ta [17], ZrO_2, Ta_2O_5 [18], MgO, SiO_2 and UO_2 [13].

The choice of technique for a binary compound such as GaAs is really limited to methods (d) and (e). The first two techniques have so far been developed only for the elements listed and the chemical etching method suffers from a general disadvantage of preferentially etching or dissolving regions of high strain, e.g. around dislocations and, in the case of III-V compounds, the rate of etching is very orientation dependent. Studies of preferential etching in InSb [19] show an increase in rate from one on a (1 1 1) surface to fifteen on a $(\bar{1}\bar{1}\bar{1})$ surface. Low energy sputtering, although a time-consuming operation, has been used in a very preliminary investigation of the range of Kr in GaAs [16]. Sputtering studies [20] indicate no significant orientation effect on rate but Anderson [21] has observed non-stoichiometric removal, with the $<\bar{1}\bar{1}\bar{1}>$ spot being slightly richer in Ga and the $<111>$ spot richer in As. The limitations and disadvantages of these methods indicate that the preferred method of layer removal from GaAs is that of vibratory polishing, as previous work with binary compounds [13] gave satisfactory results with no significant orientation dependent effect.

The vibratory polishing technique of layer removal has been described in detail previously [17] and is essentially a method of mechanically removing thin layers from the surfaces of crystals previously mounted in right cylinders of cold setting epoxy resin, which are are in turn fixed in stainless steel ballast weights. Details of the experimental conditions and the necessary precautions to be taken were also described.

In the application of ion implantation to GaAs for the formation of junction devices, the preferred dopants are the Group IIA acceptors Zn and Cd and the Group VIA donors S, Se and Te. However, for this preliminary investigation, we have chosen to use the rare gas radiotracer ^{85}Kr because, (a) it has been shown previously [18, 22] to be an immobile marker, (b) the use of a rare gas should obviate surface chemical effects and (c) it should provide information of the average mass effect as it is of intermediate mass to the dopant ions of interest viz: $16^{S^{32}}$, $30^{Zn^{65}}$, $34^{Se^{79}}$, $36^{Kr^{85}}$, $48^{Cd^{112}}$, $52^{Te^{128}}$.

2. Experimental

The GaAs specimens were cut from one large ingot grown by the static freeze technique at SERL Baldock. The ingot was undoped but n-type and measured 5×10^{16} carriers/cm^3, 0.03 Ωcm with a mobility of 4000 cm^2, V^{-1}sec^{-1}. A measure of the dislocation density was obtained by etch pit techniques which showed $\sim 10^5$ pits/cm^2.

A diamond bonded cutting wheel was used to section the ingot into slices about 1 cm $\times$ 1 cm $\times$ 0.1 cm thick. The slices of orientation $\{100\}$, $\{110\}$ and $\{111\}$ were accurately oriented to $\sim 0.5°$ and the "A" faces of the $\{111\}$ specimens (see later explanation) were positively identified by etching in 1:3 HNO_3:H_2O at 80° C for 15 sec.

The orientation of the specimens was maintained during mounting by laying them face down on plate glass with individual weights on each, then separately fixing them in cold-setting epoxy resin. The mounted specimens were then abraded and mechanically polished through various size grits down to 0.25 μm diamond, then vibratory polished in an aqueous slurry of 0.05 μm Al_2O_3 for 72 h. This treatment resulted in a flat highly polished surface which leaves no detectable damage as evidenced by reflection electron diffraction patterns. At this stage, the specimens were again X-rayed to ensure that no misorientation had taken place during the

mounting and polishing procedures.

The ^{85}Kr ions at incident energies of 10, 20 and 40 keV at various total ion doses of from 3×10^{11} to 9×10^{12} ions/cm^2 were injected into the specimens, previously masked with aluminium foil to prevent spurious edge effects, in the Harwell Mark I electromagnetic isotope separator. The beam divergence at the two higher energies was estimated to be $\sim 0.1°$ and at the lowest energy $\sim 0.3°$.

Preliminary bombardments at 40 keV showed a visible radiation damage mark appearing on the surface of the GaAs at $\sim 5 \times 10^{11}$ ions/cm^2. This mark is similar to that reported earlier in silicon [23] but is golden rather than "milky". The lowest dose to which the crystals were exposed therefore, was $\sim 3 \times 10^{11}$ ions/cm^2 in the belief that this would provide an implantation profile representative of an undamaged lattice.

The crystals of {111} orientation were implanted in the Ga side. GaAs has the zinc-blende structure, which consists of two inter-penetrating fcc sub-lattices, the Group III atom at 0,0,0 and Group V at $\frac{1}{4},\frac{1}{4},\frac{1}{4}$. Because of the two different types of atom, there is no symmetry of inversion about a point midway between any two atoms (as in the silicon diamond structure) and this gives rise to the formation of polar axes in the <111> direction. As a result of this, the surface

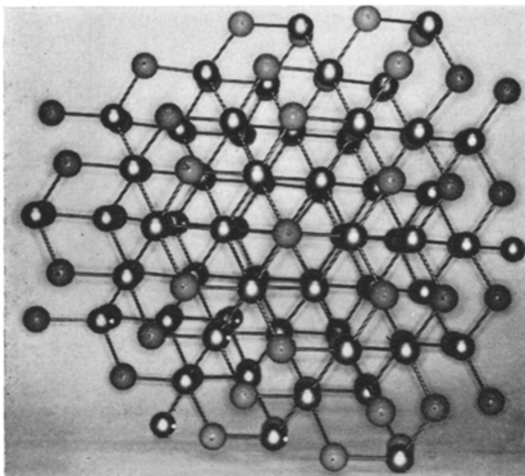

(a)

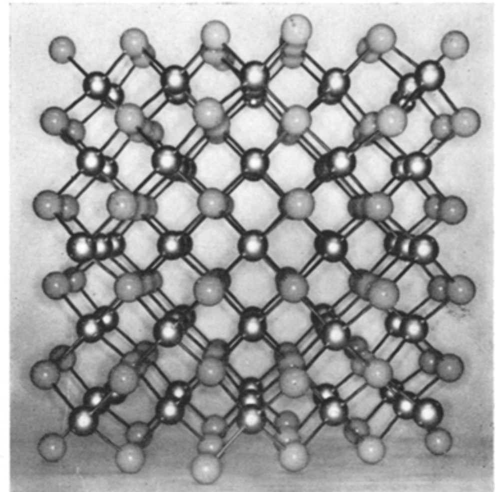

(b)

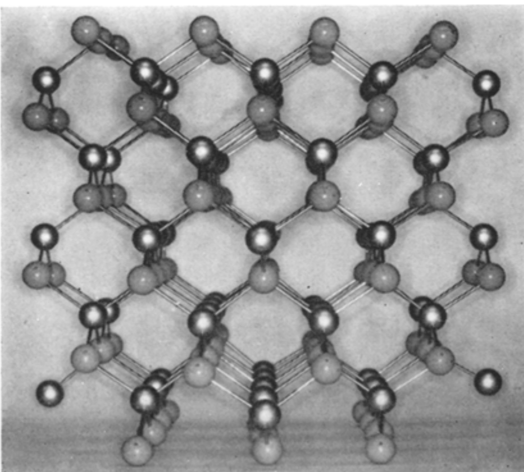

(c)

Figure 1 Model of GaAs showing the three low index directions: (a) <111>, (b) <100>, (c) <110>.

atoms of the "A" {111} face are Ga and of the opposite "B" $\{\bar{1}\bar{1}\bar{1}\}$ face are As [24]. There are many reported effects of this polarity, e.g. change in etching rate [25], anodising rate [26], so to avoid possible complications in the present work, only the "A" side was used, except where otherwise indicated. Fig. 1 shows the models of the three low index directions from which one can see the polarity effect and the increase in channel size in the order {111} → {100} → {110}.

After implantation, the residual activity of the 660 keV β of ^{85}Kr (10.3 year half-life) was measured using an end-window Geiger-Müller tube and remeasured after each layer was removed by vibratory polishing. The plot of remaining activity versus polishing time, or equivalent depth in the crystal, results in an

integral distribution curve and the results are presented in this way.

2.1. Calibration of Layer Removal

Previous calibrations of removal rate by the method of vibratory polishing have been done by weight loss [13], radioactivation analysis [17], spectrophotometry [18] and depth distribution comparisons [17]. These measurements have established that the central implanted zone of the crystal is removed at a reproducible rate and although the rate varies from one material to another, within any one material it is reproducible. It is, therefore, only the rate of removal that has to be established, although reproducibility was also checked during the course of these experiments by comparison of identical implantations in similar specimens.

The rate of removal of GaAs was measured by direct weight loss from three right cylinders of 8 mm diameter and from 1.2 to 1.8 cm length, cut with the long axes parallel to the directions <111>, <100> and <110> respectively. These right cylinders were not mounted in resin. The rate of removal was established as 5.6 ± 0.2 μg/cm^2/min of vibratory polishing time (mvp).

As the rate of removal is expected to differ from mounted to unmounted specimens, the difference was measured by injecting 40 keV ^{85}Kr into one of each type of specimen (identical dose, orientation, etc.) and sectioning them simultaneously. As expected, GaAs was removed at a faster rate from the unmounted specimen, as shown by the much shorter depth distribution, and the normalising factor required to fit the two separate curves was 3.20. The rate of GaAs removal from the mounted specimen is therefore $5.6/3.20 = 1.75$ μg/cm^2/mvp or 33 Å/mvp.

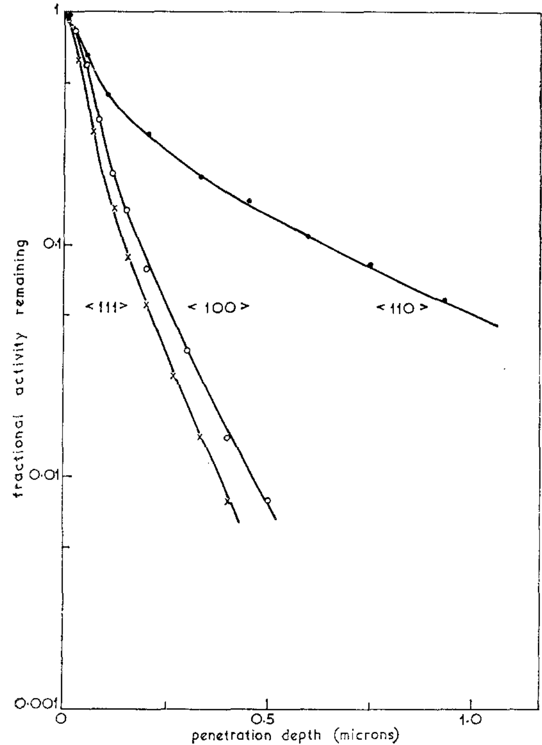

Figure 2 Effect of crystal orientation on depth distribution of 40 keV ^{85}Kr in GaAs.

3. Results and Observations

The directional dependence of 40 keV ^{85}Kr in the GaAs lattice is shown in fig. 2 and is as expected from simple considerations of the lattice transparency (cf. fig. 1), i.e. that the fraction channelled is in the order <110> > <100> > <111>. The same dependence is observed at the other energies.

The energy dependence is shown in fig. 3a-c for the three low index directions and is summarised in fig. 4 in the range-energy curves which are compared to the theoretically predicted slopes of $E^{\frac{1}{2}}$ for pure electronic stopping [27] and of E^2 for nuclear stopping [28]. The slopes of the experimental range-energy curves are seen to lie somewhere between these two values, very close to the slope of $E^{0.9}$.

The dose dependence is shown in fig. 5a-c and comparison with the depth distribution curve obtained from a pre-bombarded (10^{14} Kr^{84} ions followed by 3×10^{11} Kr^{85}) crystal shows that, as there is no further shortening of median range between the 9×10^{12} ions/cm^2 dose and the 10^{14} ions/cm^2, saturation of damage probably occurs at about the 10^{13} ions/cm^2 level. The differential form of some of the curves in fig. 5a are shown in fig. 5d.

The possibility that the shortening of range seen in fig. 5a-c may be a spurious effect, due only to an increase in rate of removal because of the gradual change from single crystal to amorphous condition, was checked in the following way: two identical <111> specimens were implanted with 3×10^{11} ^{85}Kr ions/cm^2 then one of the crystals was post-bombarded with 10^{14} stable ^{84}Kr ions/cm^2. The two crystals were sectioned simultaneously; the resultant almost identical curves are shown in fig. 6, indicating

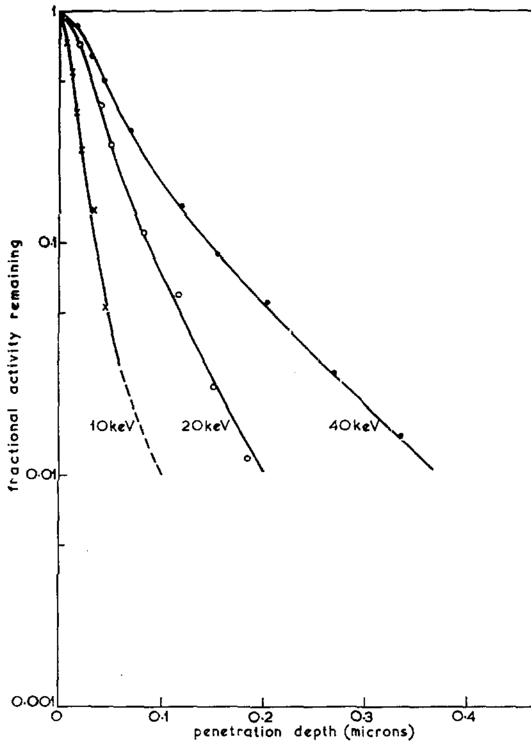

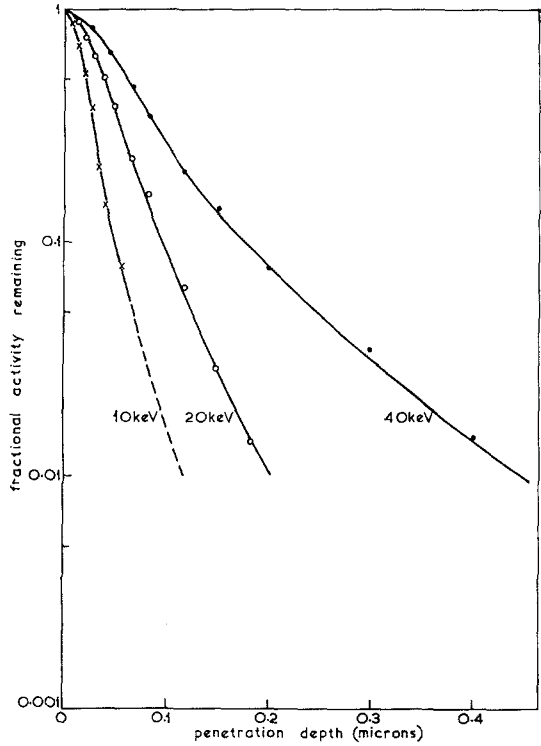

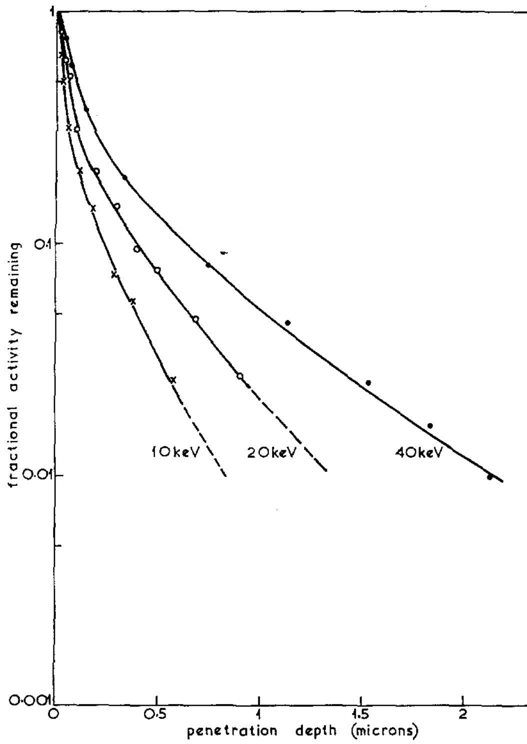

Figure 3 Effect of incident energy on depth distribution of ^{85}Kr in GaAs: (a) in <111>, (b) in <100>, (c) in <110>.

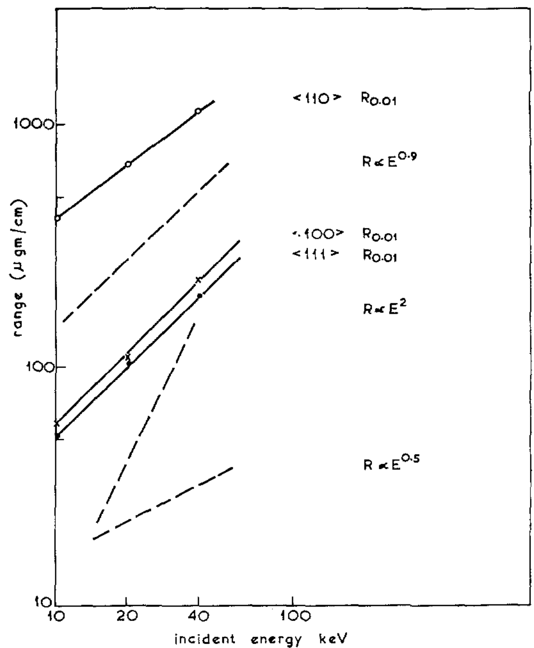

Figure 4 Range-energy relationship at the 1% of remaining activity level.

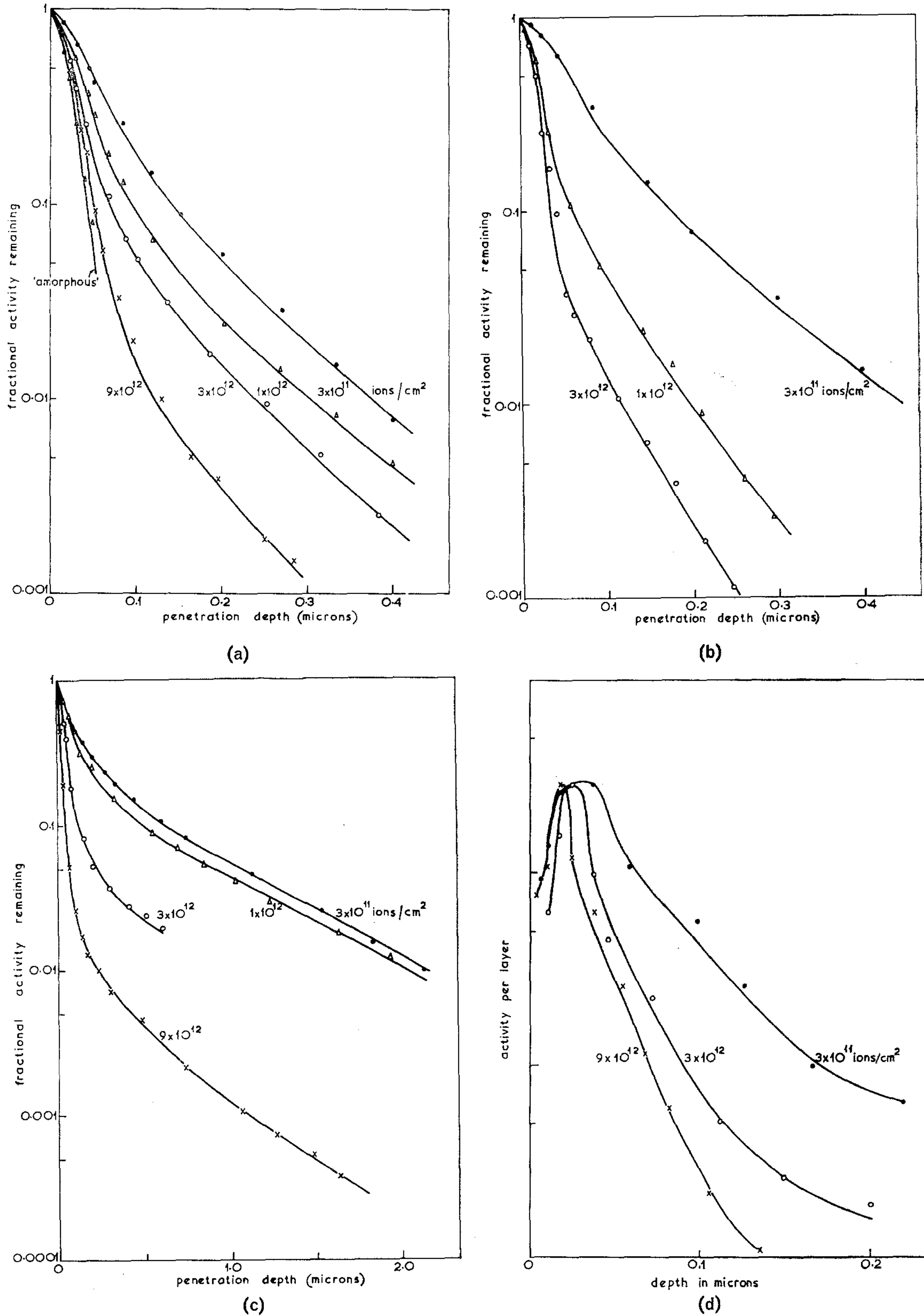

Figure 5 Effect of bombardment dose on depth distribution of 40 keV ^{85}Kr in: (a) <111>, (b) <100>, (c) <110>. (d) Differential distribution of 40 keV ^{85}Kr in <111> GaAs.

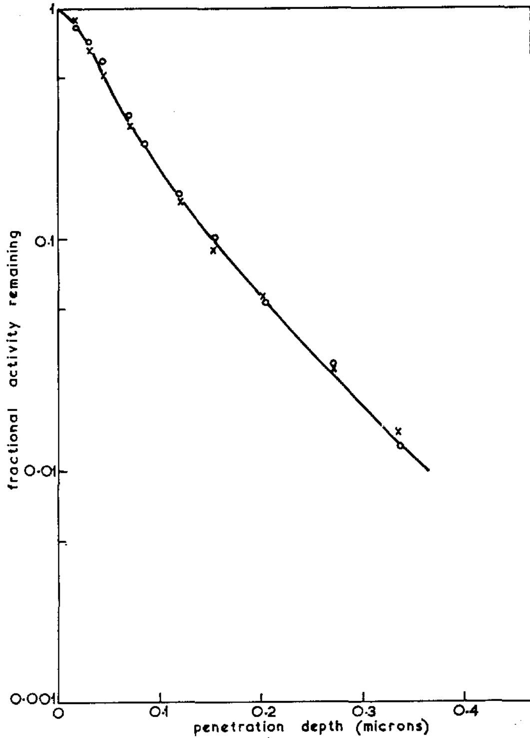

Figure 6 Effect of post-bombardment on sectioning rate of <111> GaAs: $x = 3 \times 10^{11}$ ^{85}Kr ions/cm^2; O = 3×10^{11} ^{85}Kr ions/cm^2 followed by 10^{14} ^{84}Kr ions/cm^2.

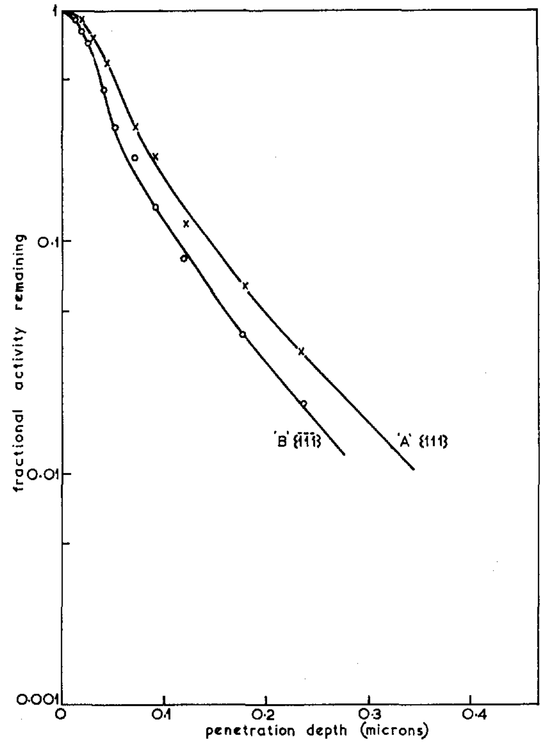

Figure 7 Effect of polarity on depth distribution of 40 keV ^{85}Kr in x="A" {111} and O="B" {$\bar{1}\bar{1}\bar{1}$} faces of GaAs.

that the rate of removal is unaffected by bombardment dose.

The effect of polarity on range was measured by injecting 40 keV ^{85}Kr into the "A" {1 1 1} face of one crystal and the "B" {$\bar{1}\bar{1}\bar{1}$} face of another. Simultaneous sectioning gave the curves shown in fig. 7; a reduction in range is seen in the "B" {$\bar{1}\bar{1}\bar{1}$} face.

4. Discussion

Previous studies [7] of the penetration of energetic heavy ions into single crystals have shown that the depth distribution curves are of two general forms. These forms are shown in fig. 8, for the case of 40 keV ^{133}Xe ions in fcc gold and bcc tungsten.

In the fcc target, the curve has two distinct parts, (1) an initial decrease due to the predominantly nuclear stopping near the surface and (2) a deeply penetrating portion made up of channelled particles. The slope of the second part gives a measure of the rate of dechannelling, i.e. the probability of a channelled ion suffering a large

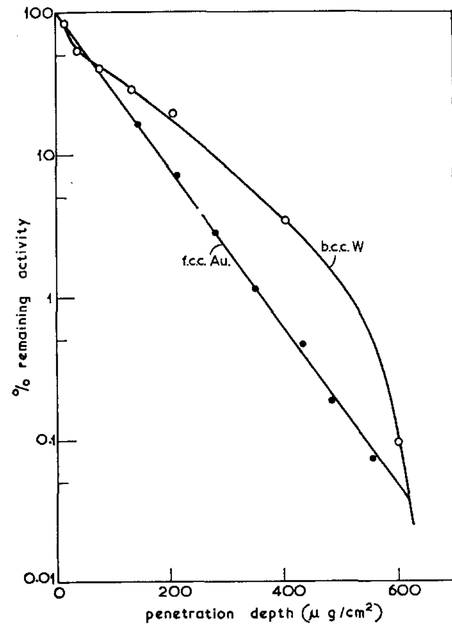

Figure 8 Depth distribution of 40 keV ^{133}Xe in fcc gold and in bcc tungsten.

angle collision and being steered out of the channel into the surrounding lattice.

In the bcc target, the curve has three parts, (1) similar to the first part of the curve in fcc targets, (2) a deeply penetrating portion made up of channelled particles but with a low rate of dechannelling and (3) a clearly defined maximum range of the channelled ions; this is determined by the rate of energy loss by electronic collision processes.

The main difference between the two forms of curve is in the fraction of incident ions reaching the maximum range. In the case illustrated (fig. 8), the fraction reaching maximum range in tungsten is $\sim 10^{-2}$ and in gold (by extrapolation) is only about 10^{-7}. This difference is believed due to the effect of atomic thermal vibrational amplitudes, generally greater in fcc than in bcc metals [7].

The form of the depth distribution curves in the present study is similar to those seen previously in fcc metals, viz a two-part curve with no sign of a maximum range. This is not unexpected as the GaAs lattice is made up of two fcc lattices and the Debye temperature of 314° K leads to a root mean square thermal vibrational amplitude $(\mu x^2)^{\frac{1}{2}}$ of 0.078 Å, comparable to that of 0.088 Å in gold at room temperature.

The similarity of depth distribution profile with that seen in gold is even more marked in the comparison of the range-energy relationships in the two cases. Fig. 4 shows an energy dependence, at the 0.01 level, of $E^{0.9}$, comparable to that of 40 keV xenon in gold of $E^{0.8}$ and is an indication that the stopping process in the channels is made up of both nuclear ($R \propto E^2$) and electronic stopping ($R \propto E^{0.5}$). The energy dependence is, therefore, that of the dechannelling process.

The measured median ranges (R_m) of 40 keV ^{85}Kr in the heavily disordered (amorphous) lattices of the <111>, <100> and <110> crystals and in the pre-bombarded <111> crystal give an average value of 10.6 ± 0.8 μg/cm^2, in good agreement with the theoretically predicted projected range (R_{proj}) of 9.5 μg/cm^2. The latter value is taken from a computer programme of Schiøtt [4] for ranges of ions in amorphous mixed substances.

This good agreement between theory and experiment is seen only in the crystals that are amorphous or nearly so. Reference to fig. 5a-c shows that the median ranges in the lightly bombarded crystals are much greater than 9.5 μg/cm^2. The discrepancy is due to the contribution from dechannelled particles, for where the true median range in amorphous material consists of the particles having nuclear encounters (i.e. not channelled), in the undamaged lattice the initially channelled but quickly dechannelled, particles add to the nuclear encounters portion, thus effectively broadening the nuclear encounter distribution. The only way therefore, of having true median ranges is by measuring the range in (a) amorphous material, (b) in crystals misoriented to give no lattice effect and (c) in an undamaged lattice where there is effectively no dechannelling of initially channelled particles [6].

The importance of dechannelling in the measurement of median ranges is illustrated in table 1, where it is seen that the greatest departure from the true R_m is at the highest energies in the most open direction and, conversely, the best fit is at the lowest energy in the least open direction.

TABLE I Comparison of measured R_m with calculated R_{proj} in "undamaged" lattice

		R_m	R_{proj}	R_m/R_{pro}
<111>	10 keV	6.9	3.5	2.0
	20	17.3	5.9	2.9
	40	23.3	9.5	2.5
<100>	10	11.2	3.5	3.2
	20	20.8	5.9	3.5
	40	33.0	9.5	3.5
<110>	10	15.6	3.5	4.5
	20	31.0	5.9	5.3
	40	48.5	9.5	5.1

The change in slope of the channelled particles (figs. 2 and 5c) also reflects the openness of the channels which, in the case of GaAs, have a ratio calculated from the unit mesh of 1:1.09:1.54 for <111> : <100> : <110>. The corresponding measured penetration at the 50% level of remaining activity is in the right order, the ratio being 1 : 1.5 : 2.1.

The effect of ion bombardment induced radiation damage in the form of shortened ranges has been observed previously for Si [10] and for MgO and SiO_2 [13]. Recent work by Nelson and Mazey [23] and Davies *et al* [31] show that the onset of damage is in the form of discrete amorphous zones of about 100 Å diameter which, as the dose is increased, overlap until a completely amorphous layer is formed. These findings are in keeping with the present observed form of range shortening which can be

interpreted as requiring a gradual transition from crystalline to amorphous over a thick region rather than a very shallow amorphous layer being formed at the onset of damage then thickening, always in the amorphous state.

The effect of polarity on range is shown in fig. 7 and is indicative of one of three possibilities, (1) that the depth of penetration is less in the "B" than the "A" face, (2) that the rate of removal is greater on "B" than on "A" and (3) that the initial depth of damage on the vibratory polished surface is greater on the "B" than the "A" face. If the third reason is valid, then it explains the first. Warekois *et al* [32] have reported greater damage in the "B" face of GaAs and InSb than in the "A" for the same treatment, although Pugh and Samuels [33] have found the same damage depth in both cases. Whatever the reason for the change in range, the discrepancy is enough to justify care being taken to identify the face being bombarded.

Finally, a comparison of the earlier data of Pöhlau *et al* [16] by sputtering methods, shows quite clearly that the doses used in their case were so high as to be of use only in measuring the amorphous range of 80 keV Kr in GaAs (fig. 9). Comparison of the channelled ranges is, therefore, not possible.

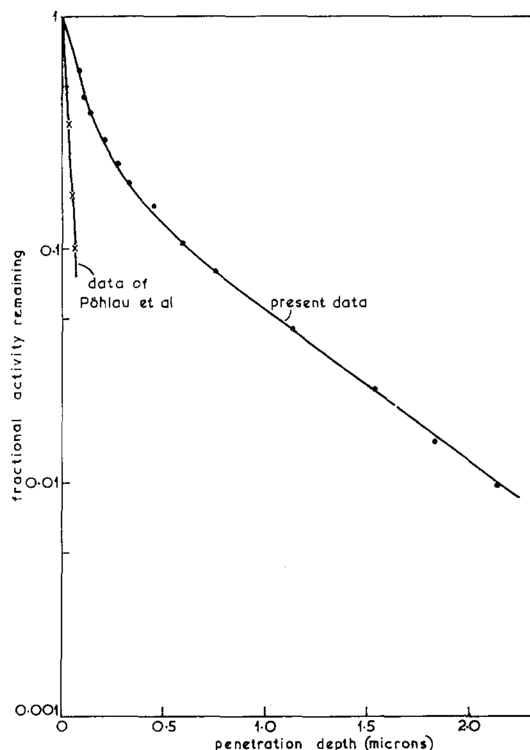

Figure 9 Comparison of present data, 40 keV ^{85}Kr in <110> GaAs with that of Pöhlau, Lutz and Sizmann, 80 keV ^{85}Kr in <110> GaAs.

5. Summary

1. A satisfactory comparison of median range with the theoretical predicted range of Kr in amorphous GaAs has been found.

2. The effect of radiation damage is very marked at relatively low ion doses, suggesting that for the introduction of high concentrations of dopant ions, simultaneous annealing with implantation will be required.

3. Maximum ranges were not measurable for the heavy ion used, confirming previous evidence that atomic thermal vibrational amplitudes play a large part in determining the chances of such a maximum range being detected.

4. The difference in range in the "A" and "B" polar faces is sufficiently great to justify proper identification of these faces.

5. The technique of vibratory polishing has been shown to be suitable for the measurement of ion ranges in GaAs. Because of the similar physical properties of the other III-V compounds, it is anticipated that the technique will be equally applicable to them.

6. The present study has provided enough information of a general kind to aid in programming implantation profiles. An extension of this is now under way to see if the use of Group II and VI dopants will result in any significant departure from the expected mass effect.

Acknowledgements

The authors are very grateful to members of SERL Baldock for providing the GaAs crystals, along with much help and advice.

This work was done under a CVD Contract and is published by permission of the Ministry of Defence (Navy Department).

References

1. "Int. Conf. on Applications of Ion Beams to Semiconductor Technology", edited by P. Glotin (Grenoble, 1967).
2. "Int. Conf. on Atomic Collisions and Penetration Studies". *Canad. J. Phys.* **46** (1968).
3. J. LINDHARD, M. SCHARFF, and H. E. SCHIØTT, *Kgl. danske Videnskab, Selskab, Mat-fys. Medd.* **33**, (1963) 14.
4. H. E. SCHIØTT. *Canad. J. Phys.* **46** (1968) 449.
5. L. ERIKSSON, J. A. DAVIES, and P. JESPERSGÅRD, *Phys Rev.* **161** (1967) 219.

6. I. M. CHESHIRE and J. M. POATE, *Phys. Lett.* **27A** (1968) 304.
7. J. L. WHITTON, *Canad. J. Phys.* **46** (1968) 581.
8. M. MCCARGO, J. A. DAVIES, and F. BROWN, *Canad. J. Phys.* **41** (1963) 1231.
9. J. A. DAVIES, J. D. MCINTYRE, R. L. CUSHING, and M. LOUNSBURY, *Canad. J. Chem.* **38** (1960) 1535.
10. J. A. DAVIES, G. C. BALL, F. BROWN, and B. DOMEIJ, *Canad. J. Phys.* **42** (1964) 1070.
11. J. L. WHITTON and J. A. DAVIES, *J. Electrochem. Soc.* **111** (1964) 1347.
12. T. ANDERSEN and G. SØRENSEN, *Canad. J. Phys.* **46** (1968) 483.
13. J. L. WHITTON and HJ. MATZKE, *Canad. J. Phys.* **44** (1966) 2905.
14. H. LUTZ and R. SIZMANN, *Phys. Lett.* **5** (1963) 113.
15. H. LUTZ, R. SCHUCKERT, and R. SIZMANN, *Nucl. Instr. Methods* **38** (1965) 241.
16. C. PÖHLAU, H. LUTZ, and R. SIZMANN, *Z. angew. Phys.* **17** (1964) 404.
17. J. L. WHITTON, *J. Appl. Phys.* **36** (1965) 3917.
18. J. L. WHITTON, *J. Electrochem. Soc.* **115** (1968) 58.
19. H. C. GATOS and M. C. LAVINE, *J. Electrochem. Soc.* **107** (1960) 433.
20. J. COMAS and C. B. COOPER, *J. Appl. Phys.* **38** (1967) 2956.
21. G. S. ANDERSON, *J. Appl. Phys.* **37** (1966) 3455.
22. J. A. DAVIES, B. DOMEIJ, J. P. S. PRINGLE, and F. BROWN, *J. Electrochem. Soc.* **112** (1965) 675.
23. R. S. NELSON and D. J. MAZEY, "Int. Conf. on Application of Ion Beams to Semi-conductor Technology", edited by P. Glotin (Grenoble, 1967).
24. E. P. WAREKOIS and P. H. METZGER, *J. Appl. Phys.* **30** (1959) 960.
25. H. C. GATOS and M. C. LAVINE, *J. Phys. and Chem. Solids* **14** (1960) 169.
26. J. F. DEWALD, *J. Electrochem. Soc.* **104** (1957) 244.
27. J. LINDHARD and M. SCHARFF. *Phys. Rev.* **124** (1961) 128.
28. C. LEHMANN and G. LEIBFRIED, *J. Appl. Phys.* **34** (1963) 2821.
29. J. L. WHITTON, *Canad. J. Phys.* **46** (1968) 581.
30. J. L. WHITTON, *Canad. J. Phys.* **45** (1967) 1947.
31. J. A. DAVIES, J. DENHARTOG, L. ERIKSSON, and J. W. MAYER, *Canad. J. Phys.* **45** (1967) 4053.
32. H. C. GATOS, M. C. LAVINE, and E. P. WAREKOIS, *J. Electrochem. Soc.* **108** (1961) 645.
33. E. N. PUGH and L. E. SAMUELS, *J. Appl. Phys.* **35** (1964) 1966.